

Acceleration of High-Energy Deuterium Ions from Laser Irradiated Foils for Stand-off Detection of Nuclear Materials

HONORS THESIS

Presented in Partial Fulfillment of the Requirements for Graduation with Honors
Research Distinction in Physics in the Undergraduate Colleges of The Ohio State
University

By:

Edward W. McCary

Project Advisor:

Dr. Richard R. Freeman, Department of Physics

© Copyright by
Edward Wright McCary
2012

Abstract

Proliferation of controlled nuclear materials poses a threat to the security of the United States. High-energy neutrons can be used in the noninvasive detection of these materials. The neutrons are generated from fusion reactions in proton rich or deuterium rich solids that are bombarded by energetic ions. Deuteron ions, accelerated from the rear-surface of laser-irradiated flat-foil targets, have been produced with energies up to 3.5 MeV. The observations were made using a Thomson Parabola Spectrometer. Deuteron ions have been accelerated from a contaminant-free layer of heavy ice coated onto the rear surface of a thin foil. Compared to earlier experiments using deuterated plastic as an deuteron source, a more than ten-fold increase in the deuteron flux was observed while the flux of contaminants was almost completely eliminated. In these experiments, the peak ion energy was observed to increase by a factor of two.

Table of Contents

| | |
|--------------------------------------------------------------|----|
| Abstract..... | i |
| List of Figures..... | iv |
| Chapters | |
| 1. Introduction..... | 1 |
| 1.1 Motivation: Active Nuclear Detection | 2 |
| 2. Ion Acceleration: Target Normal Sheath Acceleration | 3 |
| 3. Fusion as a Neutron Source | 5 |
| 4. Fusion using laser accelerated ions..... | 6 |
| 5. Methodology..... | 7 |
| 6. Results and Discussion | 11 |
| 7. Conclusion | 15 |
| 8. Acknowledgements..... | 16 |
| 9. References..... | 17 |

List of Figures

| | |
|---------------------------------------------------------------|----|
| Figure 1: Model for active scanning of cargo..... | 2 |
| Figure 2: Neutrons passing through lead shielding | 3 |
| Figure 3: Target normal sheath acceleration | 4 |
| Figure 4: Fusion illustration..... | 5 |
| Figure 5: Fusion cross sections..... | 6 |
| Figure 6: Pitcher catcher set up for fusion..... | 7 |
| Figure 7: Deuterated ice target set up | 8 |
| Figure 8: Image of cold shroud and LN2 cryogenic piping..... | 9 |
| Figure 9: Thomson parabola spectrometer (TPS) schematic..... | 10 |
| Figure 10: TPS ion spectrum | 12 |
| Figure 11: Graphs of deuterium ion and proton spectrums | 14 |

1. Introduction

Nuclear materials are playing an increasingly large role in modern day politics and they affect the lives of people around the world. As developing countries grow and expand their scientific and militaristic capabilities, proliferation of nuclear materials may pose a risk to the United States and other countries if they become available to unfriendly organizations. Fast, non-invasive and non-destructive detection, known as standoff detection, of nuclear materials is essential in insuring that enriched uranium or plutonium is not illegally transferred into or out of the US.

Traditional methods of nuclear material detection are based on the natural decay of radioactive elements. Highly enriched uranium and weapons grade plutonium have well documented emission spectra, which are easy to detect using gamma-ray scintillators and neutron detection techniques. However, these emission spectra can be significantly attenuated using the right type of shielding. This shielding of decay products poses a significant problem for the detection of weapons of mass destruction, highly enriched uranium, dirty bombs, or any other nuclear material that might be shipped into or out of the United States.

Shielding of nuclear material can be circumvented using high-energy neutrons. High-energy neutrons are useful for detecting nuclear materials; they are electrically neutral and so they only interact with atoms and molecules by elastically “bouncing off” the atomic nuclei. When a neutron bounces off of a massive nucleus, like lead, it ricochets like a billiard ball off of a bowling ball without losing much energy^[1]. This allows the neutrons to pass through dense shielding to reach the material inside.

New developments in laser technology have indicated that ultra-fast, ultra-intense lasers can be used to accelerate high-energy ions from solid foil targets. Laser accelerated ions, like deuterium, can be used to fuel a “knock-on” fusion reaction that can produce useful high-energy neutrons. The neutrons could be sent into a building or shipping container, pass through shielding, and stimulate a fission reaction by being absorbed by any fissile material inside. The decay products of nuclear materials (uranium-235, plutonium-239 etc.) are very well documented and it would be very clear if any nuclear material were inside the container.

As part of the High Energy Density Physics group at The Ohio State University I worked on the acceleration of deuterium for use in a knock-on fusion reaction. This project represents the first successful attempt at the acceleration of deuterium where the proton and carbon contamination signals are almost completely eliminated.

1.1 Motivation: Active Detection of Nuclear Material

Traditional passive detection of nuclear material relies on the detection of the natural decay of nuclear material using a radiation sensor like a Geiger counter, and is ineffective when the nuclear material is adequately shielded. Active detection boosts the radiation signal from nuclear material in order to more reliably identify dangerous materials. Active detection uses high-energy neutrons as an interrogation source, i.e. a source that stimulates fission in nuclear materials. The fission releases large bursts of radiation that can be detected using scintillators or other radiation detection devices (see Fig. 1 for a representation)^[9]. In the cases of uranium and plutonium, these neutrons will incite fission, and the resulting characteristic radiation will be detected and identified.

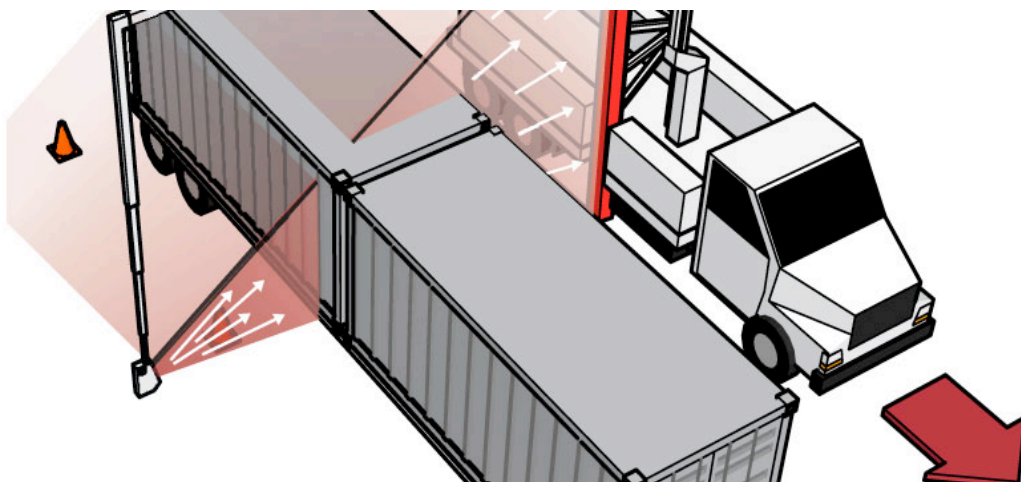


Figure 1: A model of active scanning. The white arrows at the bottom left of the picture represent the neutrons and the white arrows on the right represent the characteristic radiation being emitted and detected.

Using neutrons as the interrogation source is ideal for penetrating high-Z (large nuclei) material. Neutrons are electrically neutral, and so they do not interact electromagnetically with

electrons or protons in a shielding material. Neutrons can pass through a shield until they collide directly with a nucleus. This process allows a neutron to penetrate lead shielding; scattering elastically from nucleus to nucleus, enabling it to stimulate fission for heavily shielded material (see Fig. 2).

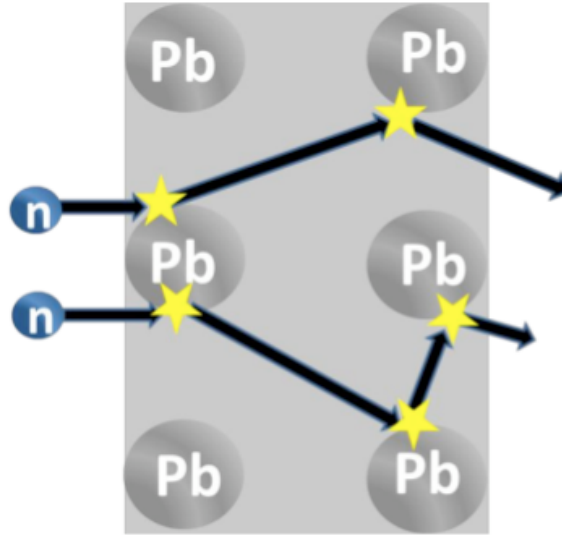


Figure 2: An illustration of energetic neutrons passing through lead shielding.

The fission releases several prompt neutrons with an average energy of .7 MeV along with two fission products, or “daughter” nuclei. The prompt neutrons are of high enough energy and are released so immediately after the fission that they are difficult to distinguish from the interrogation neutrons being used to produce the fission, so they are not ideal markers for nuclear material^[8]. Delayed radiation is a better indicator of a stimulated fission. The fission products release delayed neutrons or gamma radiation within a fraction of a second up to a minute after fission, which can be detected and easily distinguished from both natural background radiation and the interrogation source^[9].

2. Ion Acceleration: Target Normal Sheath Acceleration

The development of ultra-fast, ultra-intense lasers has opened up new frontiers in high energy density physics. With the use of lasers with intensities greater than 10^{18} Watts/cm² acceleration of protons and heavier ions by target normal sheath acceleration (TNSA) to multi-MeV energies is possible^[2,3]. In TNSA the intense laser beam is focused onto the front of a target. The laser transfers its energy into the target. The electrons are less massive than the

protons and other ions so they are accelerated faster and achieve greater speeds than the ions in the target. Some of the fast electrons escape from the target, resulting in a net positive charge on the target. This causes the remaining electrons to be trapped in a sheath at the rear target surface called the Debye sheath (see Fig. 3).

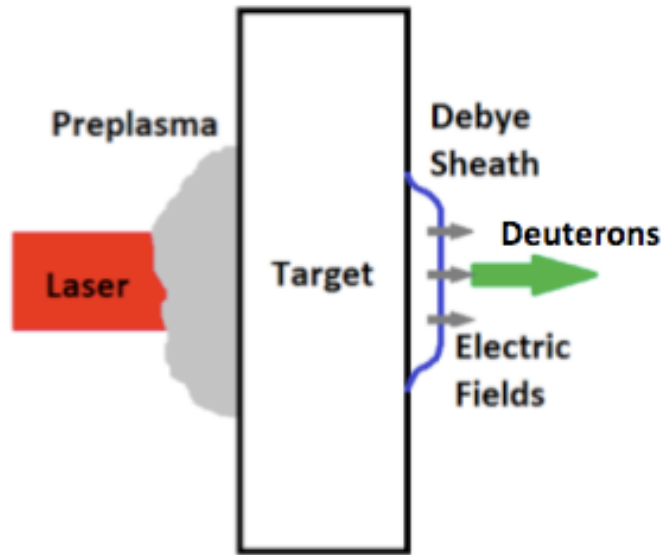


Figure 3: The laser pulse hits the front of the target creating the pre-plasma and the hot electrons. The hot electrons are driven out of the target setting up a Debye Sheath, which creates electric fields. The electric fields accelerate the deuterons. This is not to scale

The separation of the electrons in the Debye sheath and the positive ions on the rear surface sets up strong electric fields normal to the rear surface of the target^[4]. These electric fields accelerate the ions up to tens of MeV. Protons have been observed up to 58 MeV^[3]. The ions are nearly collimated, traveling with little divergence normal to the rear surface of the target. The ions are accelerated as long as the laser pulse provides electric fields, and up to the destruction of the target. Thinner targets provide higher energy ions; the thicker a target becomes, the fewer electrons escape to form the debye sheath, resulting in lower electric field strength and thus lower energy ions. The ions closest to the Debye sheath are accelerated first, and once the charge differential is diminished, the ions stop accelerating. Because of this, the final layer of the target provides the ions for acceleration^[3]. Contamination has hindered previous efforts to accelerate deuterium ions^[5]. Since the final layer of a laser target is invariably coated in contaminants from the air, proton-rich hydrocarbons and water, the accelerated ions are

dominated by this contamination layer. Protons, having the highest charge to mass ratio, comprise the bulk of the accelerated ions regardless of the target material^[6].

Several attempts at reducing the contaminate ions have been reported, with little success. Pulsed laser irradiation of the target's rear surface in an effort to increase the scale length of the plasma reduced the observed proton ion flux by two orders of magnitude; however, this was attributed to reducing the accelerating electric field at the rear surface of the target rather than eliminating the contamination. Target heating reduces the proton signal, but increases the heavier ion signal derived from the target substrate^[6].

This project represents the first successful demonstration of deuterium acceleration with negligible contamination. The accelerated deuterium originated in a layer of heavy water (D_2O) ice deposited on the rear surface of the target in vacuum, effectively burying any contamination.

3. Fusion as a Neutron Source

In order for stand-off detection of nuclear materials to be successful, compact neutrons sources are needed to interrogate the cargo. Conventional sources of neutrons use nuclear fusion fission to create high-energy neutrons. Fission plants are large, expensive, and immovable, so they do not provide an adequate source of neutrons for active detection. Fusion provides a much more attractive source. In order to induce fusion, the coulomb repulsion of the nuclei must be overcome, so that the strong nuclear force can bond the nuclei together (See Fig. 4). Neutron

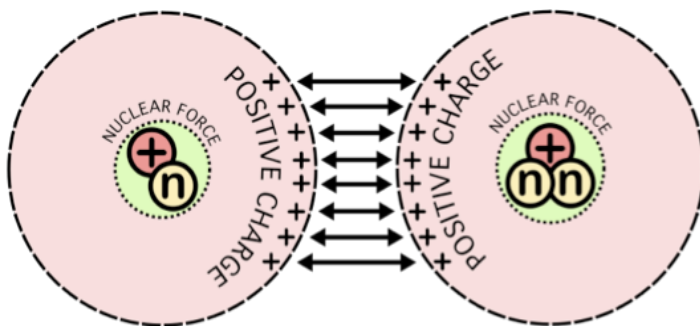


Figure 4: The shaded areas represent the area of effect for the coulomb repulsion, and strong nuclear forces.

Image courtesy of Wikipedia

sources generally rely on the deuterium-tritium $T(d,n)$ or the deuterium-deuterium $D(d,n)$ fusion reactions. Of these two, $T(d,n)$ is easier to achieve. The cross section for $T(d,n)$ cuts off just above 2 KeV of kinetic energy in the deuterium particle, and the cutoff for $D(d,n)$ fusion is at 5 KeV of kinetic energy (see Figure 5). The $T(d,n)$ and $D(d,n)$ reactions isotropically produce a 14 MeV neutron, 2.45 MeV neutron respectively, each in the center of mass frame^[7].

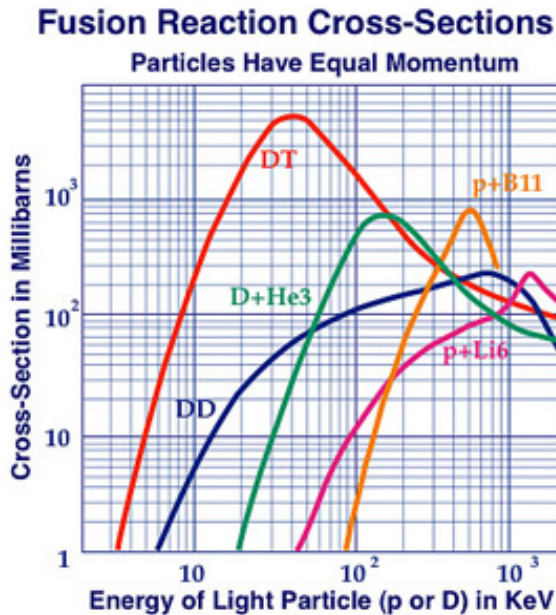


Figure 5: Fusion Cross sections as a function of lighter particle kinetic energy. The D-T fusion has the lowest cutoff, at around 2 keV. D-D has a higher cutoff, at around 5 keV.

Each of these neutrons has enough energy to penetrate cargo without being strongly absorbed into the cargo materials, and have enough energy to be absorbed by special nuclear material like uranium-235, uranium-238, or plutonium-239^[8].

While the T(d,n) reaction is easier to achieve, it has several drawbacks. Tritium is radioactive and harmful if ingested or breathed in. It is also light, so it effuses easily making it difficult to keep contained. The 14 MeV neutrons produced by the T(d,n) reaction can also be problematic when used in nuclear material detection, because they can activate common elements like oxygen. Activated oxygen will become nitrogen-16, which decays emitting a 6-7 MeV gamma ray. This high-energy gamma can mask any stimulated fission, increasing the possibility of a detector reporting a false positive or false negative^[9]. Because of the drawbacks to the T(d,n) reaction, the D(d,n) reaction provides an attractive source for neutrons to be used in stand-off detection.

4. Fusion using Laser Accelerated Ions

Laser accelerated deuterium can be used in a D(d,n) fusion reaction. Once the deuterium ions are accelerated, the simplest set up for producing fusion is the pitcher-catcher set up (see Fig. 6). The laser is focused onto a deuterium-coated target, the “pitcher”. Collimated deuterons are accelerated off of the back, where they collide with a deuterium rich “catcher” target. Within

the catcher target, the accelerated deuterium will fuse with the deuterium on the target, producing the desired high-energy neutron.

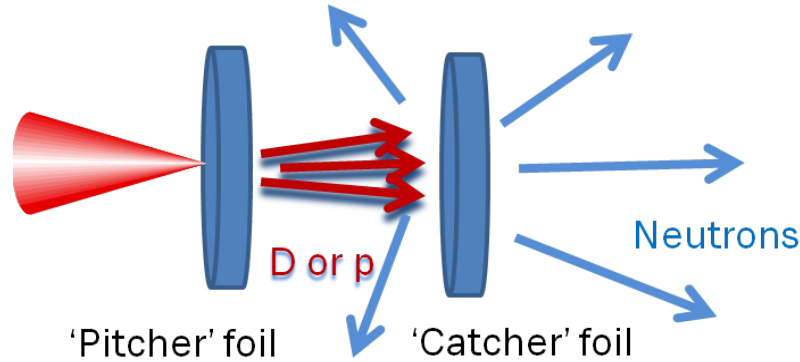


Figure 6: Neutrons are produced by accelerating ions from the pitcher foil to the deuterium rich catcher foil, resulting in a fusion reaction that produces neutrons.

In the center of mass frame of the fusion reaction, the neutrons will be released isotropically. Because the neutrons are neutral, it is impossible to collimate them into a beam using electric or magnetic fields; however, the higher the energy of the accelerated deuterons, the more collimated the neutrons become. This is a result of kinematic collimation, the faster the accelerated deuterons, the faster the center of mass frame moves, resulting in a net direction in which all the neutrons travel. Clean acceleration of deuterium makes it plausible to use lasers as the source for the deuterium to fuel the fusion reaction.

5. Methodology

This experiment was performed on the GHOST laser at the University of Texas at Austin^[10]. The GHOST laser provides about 2 J of energy in 120 fs pulses at a wavelength of 1023 nm. The laser is focused on target by an off axis parabola to a spot size of about 6 μm , corresponding to an intensity of $\sim 2 \times 10^{19} \text{ W/cm}^2$. The contrast ratio, the ratio of the pre-pulse, the result of amplified stimulated emission from the glass gain medium, to the main pulse, was 10^{-6} . The experiment was performed at a pressure of 10^{-5} Torr, or about 1.3×10^{-8} atmospheres. The targets were etched silicon wafers. The wafers had 500 nm of total thickness, 200 nm of Si_3N_4 coated with 300 nm of Aluminum. The target was a 200 μm square in the transverse

direction. The Si_3N_4 was a stopping etchant that remains after the silicon wafer was removed, and the Al was added to increase strength and to aid in target alignment via laser reflection. Figure 7 is a wafer as seen from the edge on. The laser was focused onto the etched out side of the wafer, at a 22.5° angle to the normal.

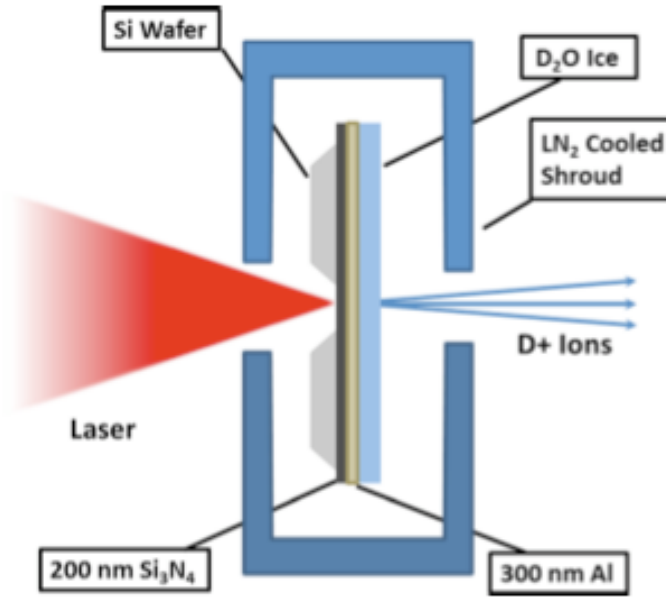


Figure 7: The $200\text{ }\mu\text{m} \times 200\text{ }\mu\text{m} \times .5\text{ }\mu\text{m}$ wafer was cryogenically cooled using liquid nitrogen to below the sublimation point for water, -130°C , then exposed to heavy water vapor just before interaction with the laser. To protect from contamination, the target was surrounded by a cryogenically cooled shroud. Figure not to scale, Courtesy of [6].

A 100 mL flask was exposed to the vacuum environment in order to evacuate the air then closed off from the vacuum chamber. From there the flask was exposed to a reservoir of heavy water, causing the flask to fill up via the heavy water's vapor pressure, 17.5 Torr at 20°C . This water vapor was then injected into the chamber and directed at the rear surface of the target by a 3 mm nozzle. The wafer cryogenically cooled to a temperature well below the sublimation point of ice, -130°C , using liquid nitrogen. Growing ice on the target usually results in crystal formation, as a result of the water beading up on the target surface before it freezes. This would result in a rough, "frosty" rear surface. A smooth surface is required in order for the sheath field to form smooth electric fields, so this would destroy any benefit by disrupting the acceleration mechanism. In order to ensure a smooth surface by preventing water nucleation on the target,

both the front and rear surfaces of the target were coated in a commercially available surfactant^[11]. The target temperature was monitored using a thermocouple. The thickness of the ice was determined by focusing a microscope that provided $\sim 2\text{ }\mu\text{m}$ spatial resolution at the rear surface of the target. A helium-neon laser was reflected off of the back of the target at an incidence angle of 11° , and standard thin-film reflectometry was used. A pattern of weak and strong reflection corresponding to a 2π phase difference in the transmitted light corresponded to a 240 nm increase in ice thickness. The number of weak and strong reflections was monitored and the ice thickness per 100 mL of water vapor at 17.5 Torr was found to be about $1.2 \pm 0.2\text{ }\mu\text{m}$. Due to the increase in the vacuum chamber pressure from releasing the water vapor, the laser could not be fired until the chamber pressure recovered.

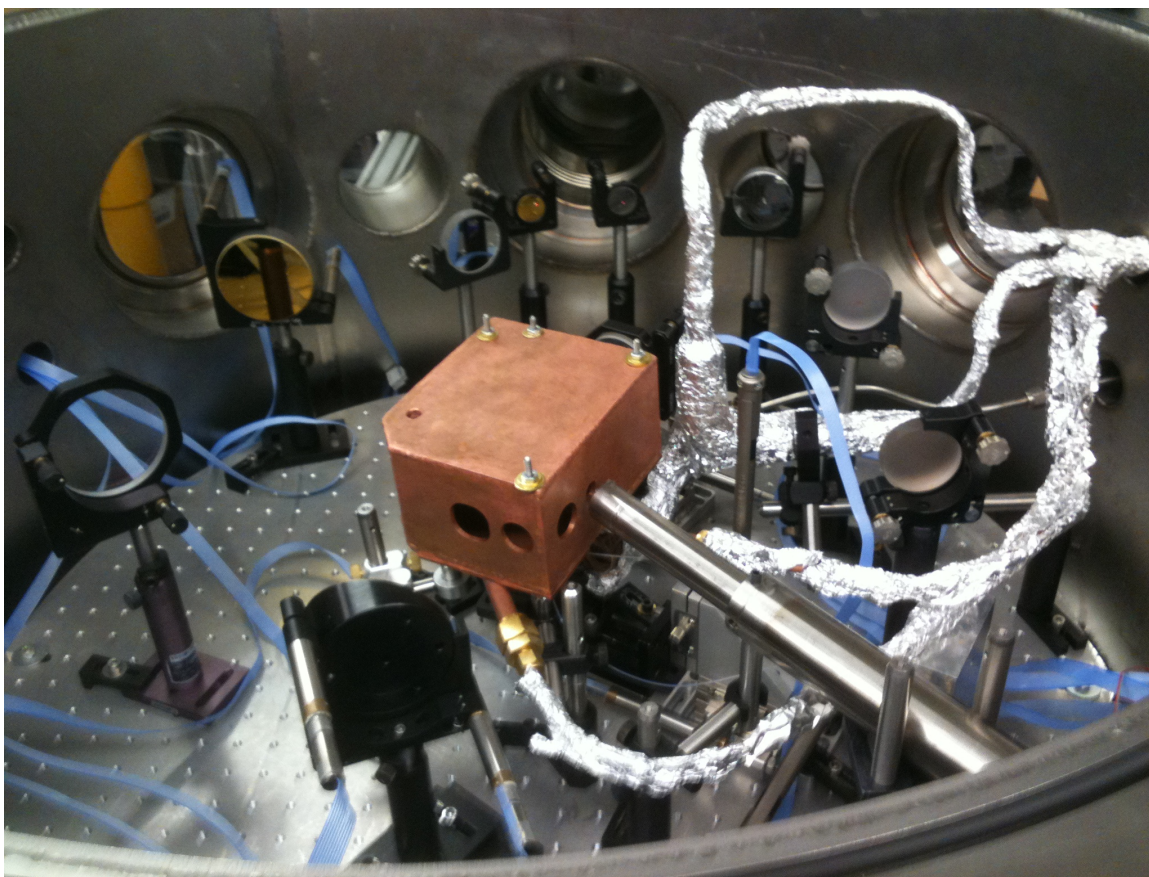


Figure 8: A picture of the final set up. The copper box is the cryogenically cooled shroud that protected the heavy water ice from any contamination while the chamber pressure recovered. The aluminum foil wrapped lines are the liquid nitrogen lines piped in from the outside of the chamber. The foil reduced the radiative heating, allowing for more efficient cooling of the target and shroud.

This was found to take ~30 seconds, during which time the ice would be subject to hydrocarbon and normal H₂O contamination. In order to reduce this contamination, a cryogenically cooled shroud, consisting of a copper box with appropriate holes drilled to allow for target positioning, laser focusing, and diagnostic line of sight was used. The shroud protected the target from any contamination proportional to the solid angle it covered. The shroud protected the target from any significant contamination during the 30 seconds it took the chamber pressure to return to 10⁻⁵ Torr. Figure 8 illustrates the final set up, showing the shroud, the liquid nitrogen lines, and some holes for diagnostics.

The ion spectrum was detected using either imaging plates or CR-39 plastic after passing through a Thomson parabola spectrometer (TPS) with a line-of-sight normal to the rear surface of the target. The TPS subtended a solid angle of 5×10^{-8} sr. The TPS consists of an electric field and a magnetic field oriented parallel to each other, and perpendicular to the path of the ions, as depicted in Figure 9. This results in a two dimensional dispersion of the ions according to their energy and their charge to mass ratio, see equation 1.

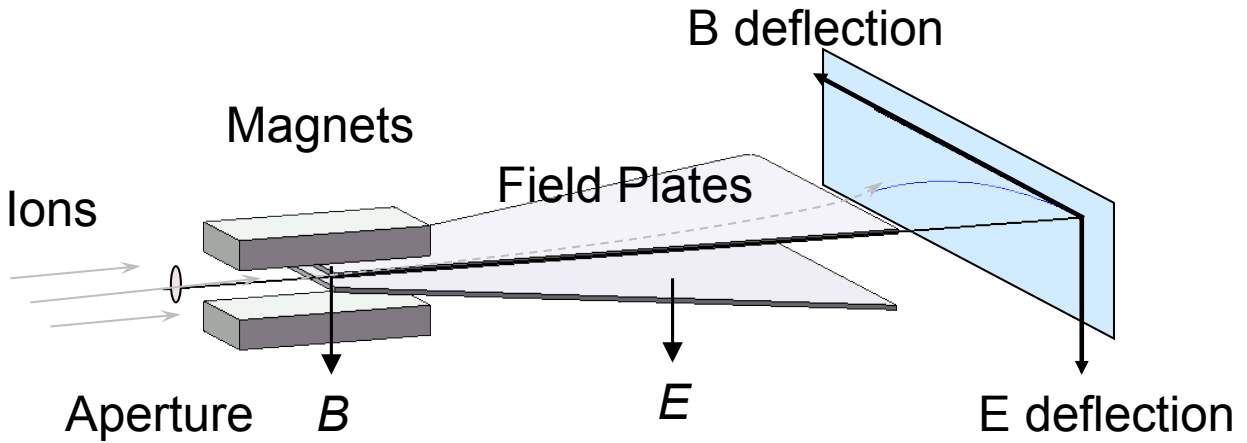


Figure 9: A representation of a TPS. The magnets provide a horizontal displacement and the Electric field provides a vertical displacement of the ions.

$$\vec{F}_{TPS} = m\vec{a} = q(\vec{E} + \vec{v} \times \vec{B})$$

$$\Rightarrow \vec{a} = \frac{q}{m}(\vec{E} + \vec{v} \times \vec{B})$$

Equation 1: A description of the forces felt by a charged particle moving through a magnetic and electric field. The final acceleration is dependent only on the charge to mass ratio of the particle, and its energy.

The energy and type of ions was determined using a MATLAB® code. A detailed description of the ion path and the TPS analysis can be found in reference [12]. On selected shots, slotted CR-39 plastic overlaid the imaging plates. The slots were 1.5 mm in diameter and spaced by 1.5mm, and were oriented perpendicular to the electric field displacement such that each slot intercepted higher and higher energy ions. Because ions interact with CR-39 by producing a visible (microscopic) damage pit, the absolute number of ions could be compared to the photo stimulated luminescence (PSL) response of the imaging plates. The Monte-Carlo code SRIM was used to determine the energy deposition per depth and energy for different ion species^[13]. The CR-39 and SRIM calibrations were used to determine the PSL response to energy and ion number, and were used to extrapolate the ion data from the imaging plates.

6. Results and Discussion

The raw accelerated ion spectra can be seen in figure 10. Figure 10(a) shows the TPS spectroscopic data for a shot where the rear surface of the target was coated with $1.2 \pm 0.2 \mu\text{m}$ of heavy water ice. The laser energy for this shot was 0.5 J on target, corresponding to a laser intensity of about 10^{19} W/cm^2 . The maximum recorded deuteron energy was 3.5 MeV. The deuterons on the rear surface of the target are much lighter than the oxygen ions (a deuteron has about 2 a.m.u. of mass, an oxygen ion has about 16 a.m.u.) and so the sheath field preferentially accelerates the deuterium ions rather than the oxygen. The negligibly weak proton and carbon signals indicate that contamination on the target was not present in any significant amount.

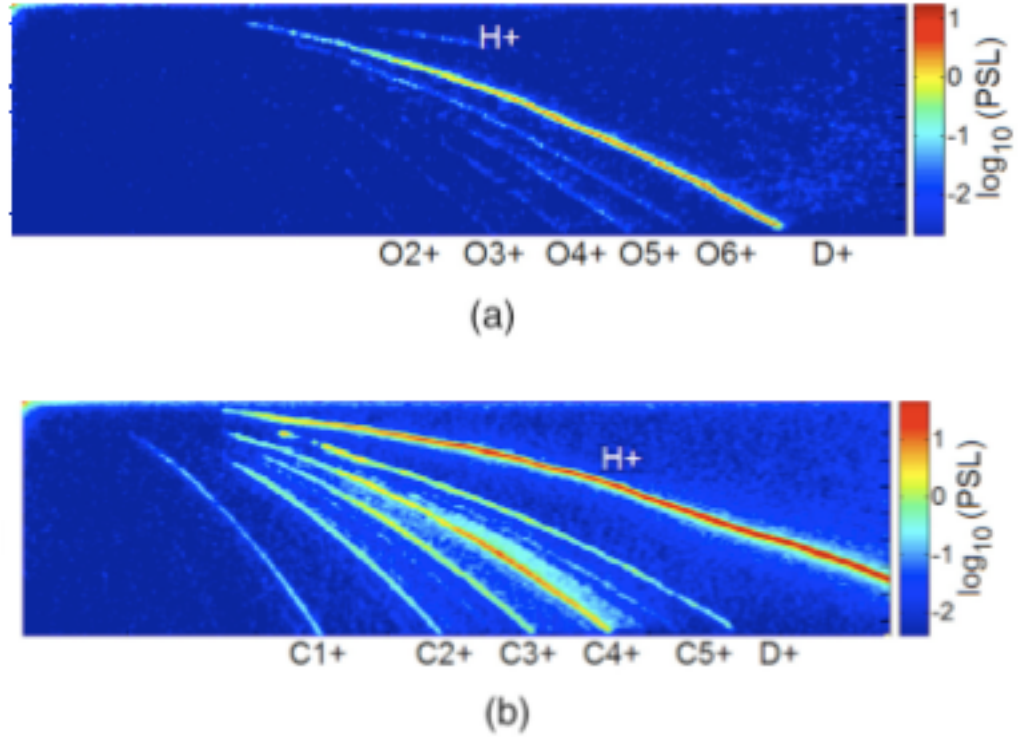
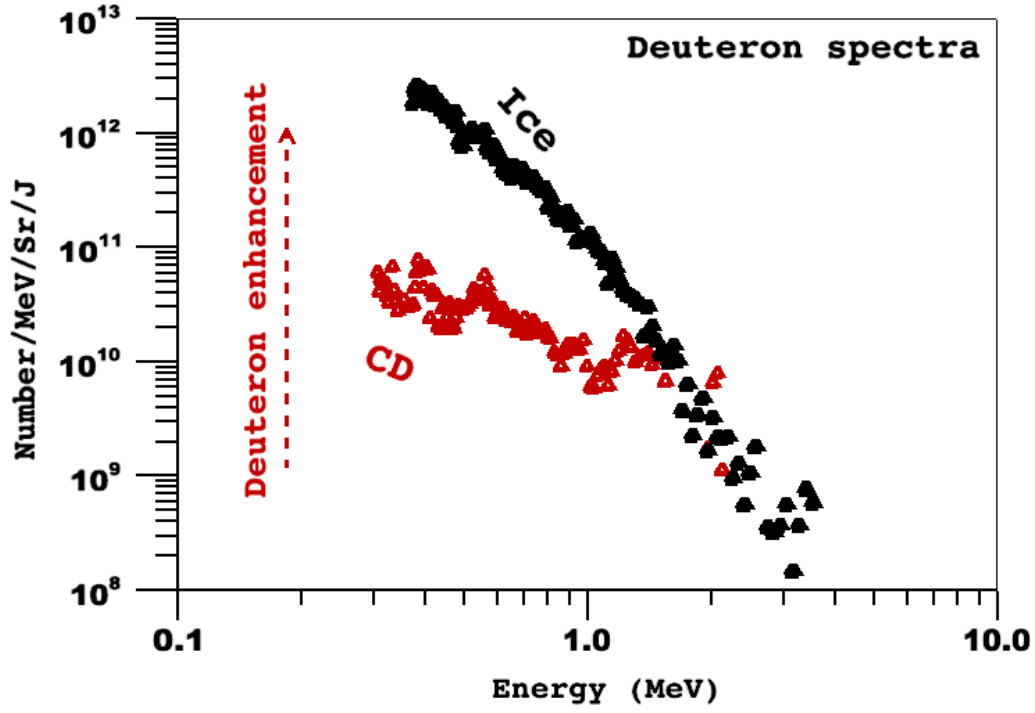


Figure 10: Comparison of ion spectra from (a) heavy ice deposition and (b) deuterated plastic (Cambridge Isotopes CD 98%) coated targets irradiated with a 1024 nm, 120 fs, 6 μm focal spot laser. (a) Ion tracks from a target coated with $1.2 \pm 0.2 \mu\text{m}$ of heavy ice, irradiated with 0.5 J of laser light, corresponding to $\sim 5 \times 10^{18} \text{ W/cm}^2$. The spectrum is dominated by deuterium ions with a maximum observed ion energy of 3.5 MeV. (b) Ion tracks from a target coated with 1 μm of deuterated plastic irradiated with $\sim 1.2 \text{ J}$ of laser light corresponding to an intensity of $1.2 \times 10^{19} \text{ W/cm}^2$. Protons, with maximum observed deuterium ion energy of 2 MeV, dominate the spectrum. Note the Logarithmic PSL scale. Image courtesy of [6].

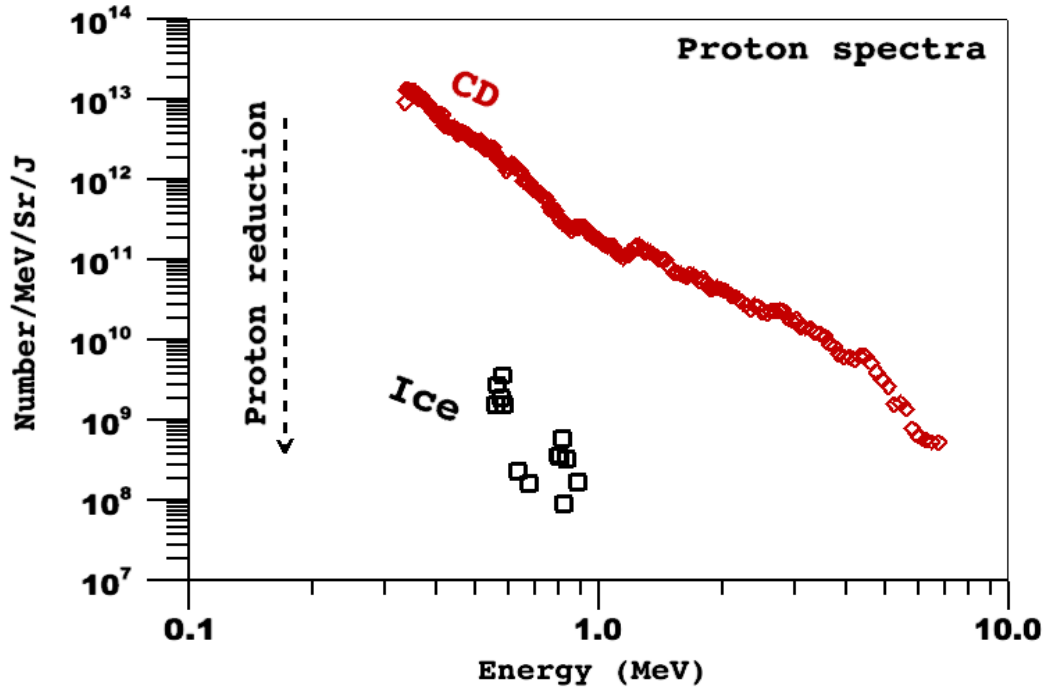
Figure 10(b) shows the TPS spectroscopic data for a target from an earlier attempt at accelerating deuterium. This target was coated in $\sim 1 \mu\text{m}$ of deuterated plastic (Cambridge Isotopes CD 98%). The CD was dissolved in toluene in a ratio of 1:150 respectively. The rear surface of the target was coated in the toluene CD solution, and upon evaporation of the toluene a $\sim 1 \mu\text{m}$ layer of CD constituted the deuterium source and target final layer. The thickness of the final layer was determined using white light interference and optical microscopy to be between 0.7 μm and 2 μm . Contamination from the air was impossible to avoid. The target was irradiated with 1.2 J of laser light corresponding to a laser intensity of $\sim 1.2 \times 10^{19} \text{ W/cm}^2$. The solid angle subtended by

the TPS in this shot was 4×10^{-7} sr. Protons and various species of carbon ions dominated the ion spectrum for the deuterated plastic case. The protons were by far the most abundant, with a maximum recorded energy of about 7 MeV. The carbon 4+ ion was the second most abundant species. The C^{4+} track seems wider than the other tracks because of unresolved oxygen lines that lie immediately adjacent to its track. In this spectrum, C^{6+} has the same TPS path as deuterium ions, because they have the same ratio. The increased brightness of the C^{6+}/D^+ line from the C^{5+} line indicates that this is in fact deuterium. A CR-39 detector indicated that there was no C^{6+} present in the track confirmed that it was left by deuterium. In this case the maximum recorded deuterium energy was 2 MeV.

Figure 11 shows the energy and number spectrum of the proton and deuterium ion tracks from figure 10. The tracks from the plastic coated targets indicate that most of the energy available to accelerate the ions is transferred into the protons, which are accelerated up to 7 MeV. The deuterium ions from the plastic target only receive up to 2 MeV of energy, and there are considerably fewer accelerated, representing a much smaller fraction of the total energy being transferred into the deuterium. In contrast the heavy ice coated target has deuterons accelerated up to 3.5 MeV and the measured proton spectrum only extends to 0.9 MeV. The deuterium ions on the ice coated spectrum represent 99% of the total ion acceleration, and are 3 orders of magnitude greater than the number of accelerated protons. This ratio of deuterons to protons is consistent with the purity of the heavy water used in this experiment, and represents a reversal in the deuterium to proton ratio in previous work^[14]. A direct comparison of the two graphs is impossible, because the laser energy in the deuterated ice case is less than half of that of the plastic coated case, but preliminary experiments performed on deuterated plastic targets with 0.5 J of laser energy indicate a proton spectrum similar to the deuterium ion spectrum we achieved with the heavy ice case.



(a)



(b)

Figure 11: Ion signal (Number/MeV/sr/J) accelerated from the target rear surface extracted from ion spectra described in Fig. 10. (a) The energy and measured number of deuterium ions accelerated from the rear surface of an ice-coated target is enhanced (black line). (b) For the ice coated targets there is a dramatic decrease in both the observed proton number and the maximum observed energy (black). (Image courtesy of [6])

The number of accelerated deuterons in the ice coated case was estimated by assuming the deuterium ions expand in a cone of half angle $\sim 10^\circ$, which is consistent with simulation^[15] and previous results accelerating protons with similar experimental parameters^[16]. The total number of forward moving deuterium ion is estimated at $\sim 1 \times 10^{11}$ deuterium ions, representing a laser conversion efficiency of about 2%. If the ice is $1.2 \mu\text{m}$ thick and we assume the ion source is $100 \mu\text{m}$ in diameter that represents 1×10^{16} deuterium atoms. It is expected that with increasing laser energy and optimized target thickness (thinner targets result in larger sheath fields as more electrons escape).

7. Conclusion

In conclusion deuterium ions were accelerated from thin metal targets coated in $1.2 \mu\text{m}$ of heavy water ice. This is the first successful attempt to accelerate deuterium ions with negligible contamination from protons and hydrocarbons. The ice deposition technique for depositing deuterium strongly favors the acceleration of deuterium over oxygen and almost completely eliminates hydrocarbon contamination. The deuterium ions are highly collimated and can plausibly be used in a “knock-on” fusion reaction in order to produce 2.45 MeV neutrons for use in non-invasive active interrogation for nuclear materials.

8. Acknowledgements

Thanks to Dr. Todd Ditmire, Dr. Aaron Bernstein, Dr. Gilliss Dyer, Sam Feldman, and the rest of the Texas Center for High Intensity Laser Science for their input and letting me use their lasers.

Special thanks to Dr. Richard Freeman, Dr. Linn Van Woerkom, Dr. Kramer Akli, Dr. Michael Storm, Dr. Enam Chowdhury, and Chris Willis at The Ohio State University for all their help, council, ideas, and overall guiding force to my work.

Extra special thanks to John Morrison for all of his work and guidance as we worked to finish both his thesis and mine.

9. References

- [1] Lamarsh, J., Baratta, A. Introduction the Nuclear Engineering. Prentice Hall, 2001.
- [2] Hatchet, S. P. et al. Electron, photon, and ion beams from the relativistic interaction of Petawatt laser pulses with solid targets. *Phys. Plasmas* 7, 2076 (2000)
- [3] Snavely, R.A et al. Intense High-Energy Proton Beams from Petawatt-Laser Irradiation of Solids. *Physical Review Letters*, **85**, 2945 (2000)
- [4] P. Mora, "Plasma Expansion into a vacuum," *Phys. Rev. Lett.* 90, 185002 (2003).
- [5] L. Willingale, G. M. Petrov, A. Maksimchuk, J. Davis, R. R. Freeman et al. Comparison of bulk and pitcher-catcher targets for laser-driven neutron production. *Phys. Plasmas* 18, 083106 (2011)
- [6] Morrison, J.T. et al. Selective deuteron production using target normal sheath acceleration. *Phys. Plasmas* 19, 030707 (2012)
- [7] National Nuclear Data Center <http://www.nndc.bnl.gov/>
- [8] Slaughter, D.R. et al. The nuclear car wash: A system to detect nuclear weapons in commercial cargo shipments. *Nuclear Instruments and Methods in Physics Research b* 241, 782 (2005)
- [9] Slaughter, D.R. et al. Detection of Special Nuclear Material in Cargo Containers Using Neutron Interrogation *Lawrence Livermore National Labs UCRL-ID-155315* (2005)
- [10] S. Feldman, in Conference on Lasers and Electro-Optics/International Quantum Electronics Conference, OSA Technical Digest (CD) (Optical Society of America, San Jose, CA, 2009)
- [11] The commercially available Rain-X® Anti-Fog™ surfactant was used.
- [12] J. T. Morrison, C. Willis, R. R. Freeman, and L. Van Woerkom, Design of and data reduction from compact Thomson parabola spectrometers. *Rev. Sci. Instrum.* 82, 033506 (2011)
- [13] J. Ziegler, J. Biersack, and U. Littmark, *The Stopping and Range of Ions in Solids* (Pergamon, New York, 1985).
- [14] B. Hou, J. Nees, Z. He, G. Petrov, J. Davis, J. Easter, A. Thomas, and K. Krushelnick, Laser-ion acceleration through controlled surface contamination. *Phys. Plasmas* 18, 040702 (2011)
- [15] Kluge, T. et al. Enhanced laser ion acceleration from mass-limited foils. *Phys. Plasmas* 17, 123103 (2010)

[16] Cowan, T.E. et al. Ultralow Emittance, Multi-MeV Proton Beams from a Laser Virtual-Cathode Plasma Accelerator. Phys. Rev. Lett. 92, 204801 (2004)